THE JOURNAL OF BIOLOGICAL CHEMISTRY VOL. 281, NO. 37, pp. 27016–27028, September 15, 2006
© 2006 by The American Society for Biochemistry and Molecular Biology, Inc. Printed in the U.S.A.

# Roles for UDP-GlcNAc 2-Epimerase/ManNAc 6-Kinase outside of Sialic Acid Biosynthesis

## *MODULATION OF SIALYLTRANSFERASE AND BiP EXPRESSION, GM3 AND GD3 BIOSYNTHESIS, PROLIFERATION, AND APOPTOSIS, AND ERK1/2 PHOSPHORYLATION**

Received for publication, May 22, 2006, and in revised form, July 10, 2006 Published, JBC Papers in Press, July 17, 2006, DOI 10.1074/jbc.M604903200

**Zhiyun Wang, Zhonghui Sun, Adrienne V. Li, and Kevin J. Yarema**[1]

*From the Department of Biomedical Engineering, The Johns Hopkins University, Baltimore, Maryland 21218*

**Roles for UDP-GlcNAc 2-epimerase/ManNAc 6-kinase (GNE) beyond controlling flux into the sialic acid biosynthetic pathway by converting UDP-GlcNAc to *N*-acetylmannosamine are described in this report. Overexpression of recombinant GNE in human embryonic kidney (HEK AD293) cells led to an increase in mRNA levels for ST3Gal5 (GM3 synthase) and ST8Sia1 (GD3 synthase) as well as the biosynthetic products of these sialyltransferases, the GM3 and GD3 gangliosides. Conversely, down-regulation of GNE by RNA interference methods had the opposite, but consistent, effect of lowering ST3Gal5 and ST8Sia1 mRNAs and reducing GM3 and GD3 levels. Control experiments ensured that GNE-mediated changes in sialyltransferase expression and ganglioside biosynthesis were not the result of altered flux through the sialic acid pathway. Interestingly, exogenous GM3 and GD3 also changed the expression of GNE and led to reduced ST3Gal5 and ST8Sia1 mRNA levels, demonstrating a reciprocating feedback mechanism where gangliosides regulate upstream biosynthetic enzymes. Cellular responses to the GNE-mediated changes in ST3Gal5 and ST8Sia1 expression and GM3 and GD3 levels were investigated next. Conditions that led to reduced ganglioside production (*e.g.* short hairpin RNA exposure) stimulated proliferation, whereas conditions that resulted in increased ganglioside levels (*e.g.* recombinant GNE and exogenous gangliosides) led to reduced proliferation with a concomitant increase in apoptosis. Finally, changes to BiP expression and ERK1/2 phosphorylation consistent with apoptosis and proliferation, respectively, were observed. These results provide examples of specific biochemical pathways, other than sialic acid metabolism, that are influenced by GNE.**

Sialic acids, 9-carbon amino-monosaccharides, are ubiquitously displayed on mammalian cell surfaces. These sugars modulate biological and pathological events ranging from development and immune function to tumor biology and the viral and bacterial infection of cells (1–3). Not surprisingly, factors that influence the biosynthesis of sialic acid-containing glycoconjugates are of great interest due to the ever growing list of cellular functions influenced by this sugar. The biochemical steps that control sialic acid production, outlined in Fig. 1, have been intensely investigated in recent years (4) with a particular focus given to the bifunctional enzyme UDP-GlcNAc 2-epimerase/ManNAc 6-kinase (GNE).[2] Whereas GNE is known to control flux into the sialic acid biosynthetic pathway through conversion of UDP-GlcNAc to ManNAc (5) and has been described as the key determinant in the surface display of sialoglycans (6), the biological activity of this protein and its impact in health and disease remain far from understood. In particular, accumulating evidence that healthy cells maintain higher levels of GNE than required for sialic acid production raises the possibility that GNE may be a "moonlighting" protein that serves multiple functions within a cell (7, 8).

The hypothesis that cells have "excess" GNE is based on two human diseases that suffer from single amino acid mutations in this protein. The first, sialuria, is a rare congenital disorder characterized by mutations in the regulatory domain of GNE (9) that alleviate the allosteric feedback inhibition that normally occurs upon binding of the downstream metabolite CMP-Neu5Ac (Fig. 1) (10). As a result, GNE-catalyzed conversion of UDP-GlcNAc to ManNAc greatly increases, and cytosolic levels of sialic acid rise dramatically (by ~70–200-fold (11)). Because this increase occurs without a corresponding change in the copy number of GNE (12) or an increase in UDP-GlcNAc (the already abundant substrate of this enzyme), it is a reasonable hypothesis that normal cells have the requisite metabolic machinery (*i.e.* enzymes and small molecule substrates) in place to produce much higher levels of sialic acid than they require. The presence of the large pool of UDP-GlcNAc found in cells can be rationalized by considering the several biochemical pathways that use this compound. For example, UDP-GlcNAc is used as an activated sugar donor for glycosylation (13); it is

* This work was primarily supported by the Advancement for Research in Myopathies (ARM) Foundation. Funding from National Institutes of Health Grant 1R01CA112314-01A1 was used for the ERK1/2 phosphorylation studies, and funding from National Science Foundation Grant QSB-0425668 was used for the RT-PCR analysis of sialic acid-processing enzymes. The costs of publication of this article were defrayed in part by the payment of page charges. This article must therefore be hereby marked "*advertisement*" in accordance with 18 U.S.C. Section 1734 solely to indicate this fact.

[1] Supported by the Arnold and Mabel Beckman Foundation. To whom correspondence should be addressed: The Johns Hopkins University, Clark Hall 106A, 3400 N. Charles St., Baltimore, MD 21218. Tel.: 410-516-4914; Fax: 410-516-5182; E-mail: kyarema1@jhu.edu.

[2] The abbreviations used are: GNE, UDP-GlcNAc 2-epimerase/ManNAc 6-kinase; HIBM, hereditary inclusion body myopathy; qRT-PCR, quantitative real-time polymerase chain reaction; shRNA, short hairpin RNA; siRNA, small interfering RNA; shGNE, short hairpin GNE; RNAi, RNA inhibition; MAPK, mitogen-activated protein kinase; MTT, 3-(4,5-dimethylthiazol-2-yl)-2,5-diphenyltetrazolium bromide; rGNE, recombinant GNE; GM1, Gal$\beta$3GalNAc$\beta$4(Neu5Ac$\alpha$3)Gal$\beta$4GlcCer; GM2, GalNAc$\beta$4(Neu5Ac$\alpha$3)Gal$\beta$4GlcCer; GM3, Neu5Ac$\alpha$3Gal$\beta$4GlcCer; GD3, Neu5Ac$\alpha$8-Neu5Ac$\alpha$3Gal$\beta$4GlcCer.



This is an Open Access article under the CC BY license.

converted to a second sugar donor, UDP-GalNAc (13); and it is used as a substrate for *O*-GlcNAc protein modification (14, 15). By contrast, the presence of "excess" GNE, whose enzymatic activity is largely kept quiescent through feedback inhibition in healthy cells, as well as tissue-specific splice variants that have no clear impact on sialic acid production (16, 17) has been puzzling but could be explained by the notion that this protein has roles other than catalyzing the first two steps of sialic acid biosynthesis.

The hypothesis that GNE has cellular functions beyond sialic acid production has been reinforced by sialic acid metabolism in hereditary inclusion body myopathy (HIBM), a late onset congenital disorder affecting skeletal muscle. Genetic evidence has linked HIBM to single amino acid mutations (18, 19) scattered throughout both catalytic domains of GNE (20). These mutations reduce the ability of GNE to convert UDP-GlcNAc to ManNAc by as much as 70–90% in cell-free assays (21, 22). Contrary to these *in vitro* findings, which would be expected to translate into reduced sialic acid production by reducing metabolic flux into the biosynthetic pathway for this sugar (Fig. 1), are studies that show that HIBM patients have approximately normal levels of sialic acid (23, 24). Even if a small subset of glycans crucial for muscle function, such as $\alpha$-dystroglycan, experience anomalous sialylation in HIBM and are responsible for disease symptoms (25) (although evidence also exists to the contrary (26)), it is now clear that overall production of sialic acid is not significantly reduced in this disease. The apparent disconnect between *in vitro* results and sialic acid production in HIBM patients can be resolved by considering the lesson learned from sialuria that cells have an excess of GNE beyond the amount required to supply flux into the sialic acid pathway. Consequently, it is reasonable to postulate that the "residual" enzymatic activity of GNE in HIBM patients is comparable with healthy cells after CMP-Neu5Ac-mediated feedback inhibition has been considered. These considerations supply a mechanistic explanation for the nearly normal levels of sialic acid found in HIBM patients but leave the biochemical basis of cellular abnormalities found in HIBM unanswered. The hypothesis that GNE has a second role, beyond supplying metabolic flux into the sialic acid pathway, opens the door to the possibility that a defect in this currently unknown activity is responsible for HIBM symptoms.

Reports that GNE shuttles to and from parts of the cell not involved in sialic acid metabolism (27) provide clues to a second cellular role for this protein. In particular, the presence of GNE in the nucleus, where it is not required for ManNAc production, raises the intriguing possibility that this protein regulates gene expression. Accordingly, we investigated whether the role of GNE in sialylation, supplying the metabolic pathway responsible for the synthesis of activated sugar CMP-Neu5Ac, could be augmented by modulating the expression of sialyltransferases, the set of ~20 biosynthetic enzymes that work in parallel to install terminal Neu5Ac residues onto underlying oligosaccharide structures (Fig. 1). As described in this report, we found that overexpression of recombinant GNE and inhibition of endogenous GNE by RNA inhibition (RNAi) methods influenced the expression of ST3Gal5 (GM3 synthase) and ST8Sia1 (GD3 synthase) and resulted in corresponding changes to the biosynthetic products of these sialyltransferases, the GM3 and GD3 gangliosides. Moreover, the manipulation of GNE had an impact on proliferation and apoptosis consistent with the known cellular effects of these gangliosides. Finally, biochemical mechanisms for the ganglioside-mediated effects of GNE on proliferation and apoptosis were identified and occur, at least in part, through the phosphorylation of ERK1/2, an important element of MAPK signaling pathways and through the BiP-associated unfolded protein response, respectively.

## EXPERIMENTAL PROCEDURES

*Cell Lines and Culture Conditions*—The human epithelial kidney cell line (HEK AD293) was obtained from Stratagene (La Jolla, CA) and was cultured in a 37.0 °C, water-saturated, 5.0% carbon dioxide incubator in medium specified by the ATCC (Dulbecco's modified Eagle's medium supplemented with 10% fetal bovine serum and the concentration of penicillin/streptomycin specified by the supplier (Sigma). The SK-MEL-28 cell line was obtained from the ATCC (Manassas, VA) and cultured following published conditions (28). D(+)-Glucosamine also was purchased from Sigma. Fetal bovine serum was from Hyclone Laboratories (Logan, UT). The human embryoid body-derived (hEBD LVEC) line was kindly provided by the Shamblott Laboratory (The Johns Hopkins Medical Institute, Baltimore, MD) and was cultured following published conditions (29).

*Cloning of GNE and the Construction of Expression Vectors*—The GNE gene was amplified by PCR by using primers AAA-CTCGAGATGG AGAAGAATGGAAATAACC (the XhoI restriction site is underlined) and TTTAAGCTTGTAGATC-CTGCCTGTTGTGTAG (HindIII). PCR products were digested by XhoI and HindIII endonuclease (New England Biolabs, Beverly, MA), purified by agarose gel electrophoresis and ligated in-frame into the pcDNA3.1 vector (Invitrogen) with T4 DNA ligase. Plasmids were routinely amplified in the *Escherichia coli* DH5$\alpha$ strain and isolated from cultures by using the Qiagen Plasmid Spin Midiprep Kit (Qiagen, Valencia, CA). The R266Q and R266W GNE mutants were created by site-directed mutagenesis with the mutagenic oligonucleotides 5′-GGT-TCGAGTGATGCAGAAGAAGGGCATTGAGCA-3′ and 5′-GGTTCGAGTGATGTGGAAGAAGGGCATTGAGCA-3′ for the R266Q and R266W sialuria mutations, respectively (where the site of mutation is underlined) through PCR-like amplification with Pfu polymerase. PCR was performed for 14 cycles by the following program for each cycle: denaturation at 95 °C for 30 s, annealing at 55 °C for 1.0 min, and extension at 68 °C for 10 min. The parental template was then digested specifically by the restriction enzyme DpnI, which cuts only dam-methylated DNA. The nicked plasmid vector pcDNA3.1 (Invitrogen), with the desired mutations, was then transfected into *E. coli* 5$\alpha$. All mutant constructs were sequenced by the DNA Analysis Facility Finch-Server (The John Hopkins University, Baltimore, MD).

*Determination of the Sialic Acid Content of GNE-transfected Cells*—HEK 293 cells were transfected with the mutant or wild-type forms of GNE shown in Fig. 3 by the Lipofectamine 2000 method (Invitrogen) following the manufacturer's instructions. The transfected cells were incubated for 24 h to allow expres-

sion of GNE. The complete medium (with 5.0% fetal bovine serum) was then replaced with serum-free Dulbecco's modified Eagle's medium and supplemented with 2.0 mM D(+)-glucosamine. Glucosamine was added to increase metabolic flux through the hexosamine pathway (15), ensuring that a lack of UDP-GlcNAc did not hinder the production of ManNAc (12). ManNAc produced by GNE subsequently intercepts the sialic acid pathway (see Fig. 1) and increases total cellular levels of sialic acid; in this study, sialic acid levels were measured by an adaptation of the periodate/resorcinol method (30, 31). In brief, after the cells were incubated with glucosamine for 24 h, they were harvested by trypsinization and counted with a Coulter Z2 instrument. The cells were then washed by pelleting by centrifugation (at 900 × *g* for 2.0 min) followed by resuspension in 1.0 ml of phosphate-buffered saline by repeated, but gentle, pipetting. This step was repeated two times to ensure that residual serum proteins, which are rich in sialoglyconjugates, were removed. The cells were resuspended in 250 μl of phosphate-buffered saline and then lysed by three freeze/thaw cycles. In order to quantify sialic acid, the sample was oxidized by the addition of 5.0 μl of 0.4 M periodic acid followed by incubation on ice for 1.5 h, followed by 15 min of boiling in 500 μl of 6.0% (w/v) resorcinol, 2.5 mM $CuSO_4$, 44% (v/v) concentrated HCl. After cooling, 500 μl of *t*-butyl alcohol was added to each sample. The samples were vortexed and centrifuged at 15,700 × *g* for 5.0 min to pellet insoluble cell debris. Immediately after spinning, the supernatants were decanted into the cuvettes, and optical density readings were taken at 630 nm. Sialic acid concentrations were calculated by comparison of these optical density values with a standard curve generated from known concentrations (0, 5.0, 10, 25, 50, 100, 150, 200, and 250 μM) of sialic acid. Data are expressed in molecules of sialic acid/cell (in all cases, cells were enumerated by Coulter Z2 cell counter analysis before lysis). Chemical reagents used in these assays, including copper sulfate, resorcinol, periodic acid, and hydrochloric acid, were from EM Sciences (Gibbstown, NJ).

*Real-time PCR Quantification of Gene Expression*—The mRNA levels of the sialic acid-processing genes listed in Table 1 were analyzed by the quantitative real-time polymerase chain reaction (qRT-PCR) method. In addition, the two housekeeping genes glyceraldehyde-3-phosphate dehydrogenase and β-glucuronidase (32) were monitored in each experiment. Primers, also listed in Table 1, were designed by using the Primer3 software (available on the World Wide Web at www.broad.mit.edu/cgi-bin/primer/primer3_www.cgi/) (33) and were obtained from MWG-Biotech (High Point, NC).

The basic protocol followed for qRT-PCR experiments began with the isolation of total RNA from 5.0 × $10^6$ cells with the RNeasy Mini Kit (Qiagen, Valencia, CA) or by the TRIzol (Invitrogen) method. RNA quality was assessed by agarose gel electrophoresis (1.8% gels run with TAE buffer followed by nucleic acid band visualization under UV illumination after ethidium bromide staining) and quantified by $A_{260}/A_{280}$ OD readings. RNA integrity was confirmed using 18 S rRNA primers, and samples were standardized based on equal levels of β-actin cDNA. Quantitative real-time PCR was performed in an ABI Prism 7000 sequence detector (Applied Biosystems) using SYBR Green PCR Master Mix reagent (Applied Biosystems). Reactions were performed in 20 μl of a mixture containing a 2.0-μl cDNA dilution, 1.0 μl (10 pmol/μl) of primers, and 10 μl of 2× SYBR master mix containing Amplitaq Gold DNA polymerase, reaction buffer, a dNTP mixture with dUTP, passive reference, and the SYBR Green I. PCR conditions were as follows: one cycle of 2.0 min at 50 °C, 95 °C for 10 min, followed by 40 cycles of 95 °C for 15 s and 60 °C for 1.0 min. Specific PCR products were detected with the fluorescent double-stranded DNA binding dye, SYBR Green (34). PCR amplification was performed in triplicate and replicated in three independent experiments. Gel electrophoresis and melting curve analyses were performed to confirm correct PCR product sizes and the absence of nonspecific bands. The expression levels of each gene were normalized against β-actin using the comparative CT method according to the manufacturer's protocols (75).

*Analysis of Cell Surface and Total Levels of GM3 and GD3*—The method for the analysis of cell surface GM3 and GD3 expression by flow cytometry was adapted from published protocols (28, 35). Briefly, these tests were performed by detaching SK-MEL-28 or GNE-transfected HEK AD293 cells by trypsinization and washing them with washing buffer (1.0% bovine serum albumin, 0.1% $NaN_3$ in phosphate-buffered saline). Cells (1.0 × $10^6$) were stained with 20 μg/ml of a mouse monoclonal antibody against GM3 (NBT-M101/M102, isotype IgM, clone M2590; Cosmo Bio Co., Ltd., Tokyo, Japan) and detected with fluorescein isothiocyanate-conjugated Affinipure rabbit anti-mouse IgM (Jackson Immunoresearch, West Grove, PA). The same procedure was used for GD3 analysis, except cells were stained with mouse anti-human ganglioside GD3 monoclonal antibody (Product number 371440, clone 110.14F9, isotype IgG3; Calbiochem) diluted 1:50 in washing buffer and detected with a donkey anti-mouse IgG antibody conjugated to fluorescein (Jackson Immunoresearch). Control samples stained with secondary antibody alone were analyzed in parallel in each experiment. Samples were analyzed with a FACScan flow cytometer and Cell Quest software (BD Immunocytometry Systems, San Diego, CA), and a minimum of 5000 events were acquired for each sample. Analysis of total (*i.e.* surface and intracellular) GM3 and GD3 was tested in fixed and permeabilized cells (36) by adaptation of a method used to quantify intracellular levels of $p21^{WAF1}$ (37). Briefly, before completing the staining procedure described above, cells were fixed by incubation in 4.0% paraformaldehyde in phosphate-buffered saline for 10 min at room temperature followed by permeabilization in a buffer containing 0.5% Triton X-100 for 2.0 min at room temperature.

*Preparation and Transfection of Short Hairpin RNAs (shRNAs) and Small Interfering RNAs (siRNA)*—GNE-specific and control shRNA expression vectors were produced and purified by using the MessageMuter™ shRNA interference production kit (Epicenter® Biotechnologies, Madison, WI). Three shRNA GNE-specific sequences were selected with the online siMAX™ design tool MWG-Biotech (High Point, NC) and cross-referenced with the National Center for Biotechnology Information data base (available on the World Wide Web at www.ncbi.nlm.nih.gov/BLAST/) to ensure that only the GNE gene was targeted. These sequences were 5′-AGATTACATTGTTGCACTA-3′ (shGNE760), 5′-TTAACATTGGATG-

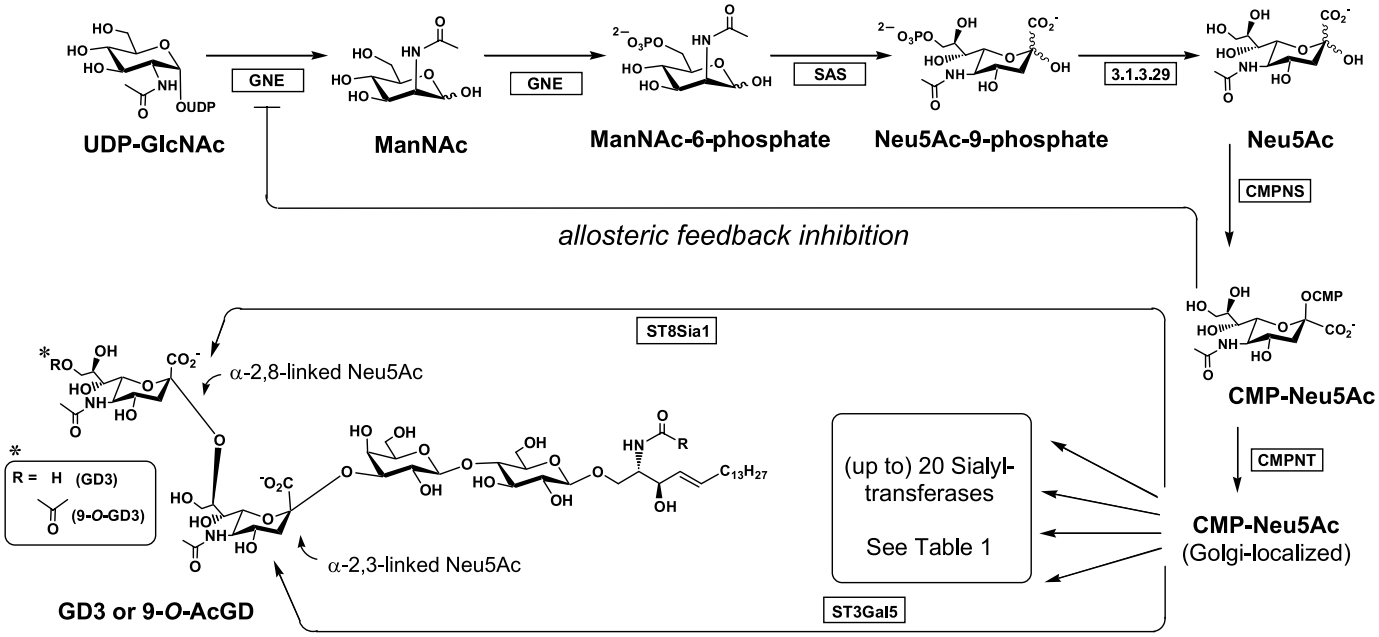


FIGURE 1. **The sialic acid biosynthetic pathway.** GNE catalyzes the conversion of UDP-GlcNAc to ManNAc as well as the phosphorylation of the C-6 hydroxyl group of ManNAc. ManNAc-6P is then sequentially converted to CMP-Neu5Ac and transported into the lumen of the Golgi, where one of ~20 human sialyltransferases use this activated nucleotide sugar to install a sialic acid residue onto a glycoprotein or a glycolipid. In the example shown, ST3Gal5 and ST8Sia1 convert LacCer into ganglioside GD3 by the stepwise addition of α-2,3- and α-2,8-linked sialic acids. The full names and complete list of human sialyltransferases and pathway enzymes are given in Table 1.

CACTTA-3′ (shGNE827), and 5′-CCTATGAAGAGAGGATTAA-3′ (shGNE1448) based on GenBank™ NM_005476 nucleotide sequences 760–778, 827–845, and 1448–1466, respectively. The DNA oligonucleotides required for shGNE synthesis (5′-AAGGAGATTACATTGTTGCACTACTTGCTTCTAGTGCAACAATGTAATCTCCTATAGTGA-3′ (shGNE760), 5′-AAGGTTAACATTGGATGCACTTACTTGCTTCTAAGTGCATCCAATGTTAACCTATAGTGA-3′ (shGNE827), and 5′-AACCTATGAAGAGAGGATTAACTTGCTTCTTAATCCTCTCTTCATAGGTATAGTGA-3′ (shGNE1448)) were synthesized by MWG-Biotech (High Point, NC), and shRNA-targeting luciferase (shRNA-luc) was used in transfection (*i.e.* "negative") control samples. In addition to these three shRNAs, siRNA targeted against the 760 region of GNE (*i.e.* the 5′-AGATTACATTGTTGCACTA-3′ sequence) was tested by using sense siRNA GNE 760 5′-AGAUUACAUUGUUGCACUATT-3′ and antisense siRNA GNE760 5′-UAGUGCAACAAUGUAAUCU-3′ (Ambion, Inc., Austin, TX). For siRNA experiments, the transfection control was the Ambion Silencer™ Negative Control 1 siRNA (catalog number 4611). In each case, HEK AD293 cells were plated at density of $4.0 \times 10^5$ cells/well in 6-well tissue culture plates and 24 h later were transfected with 20 nM shRNA or 20 nM siRNA using siPORT™ amine (Ambion Inc., Austin, TX) according to the manufacturer's protocol. Forty-eight hours after transfection, RNA was extracted from the cells, and levels of mRNA for GNE, ST8Sia1, and ST3Gal5 were analyzed with real-time PCR as described above.

*Western Blot Analysis*—An equal amount of protein from each sample (40 μg) was incubated for 5.0 min at 100 °C in Laemmli buffer (Bio-Rad), separated on an 11% SDS-polyacrylamide discontinuous gel, and then electrophoretically transferred to a nitrocellulose membrane (Bio-Rad). The membrane was blocked with Tris-buffered saline containing 5.0% nonfat milk and 0.1% Tween 20 for 1.0 h at room temperature and then incubated overnight with rabbit phospho-p44/42 MAPK monoclonal antibody and p44/42 MAPK antibody (1:1000 dilution) (Cell Signaling Technology, Beverly, MA) at 4.0 °C, followed by anti-rabbit IgG, horseradish peroxidase-linked antibody (1:2000) for 1.0 h. Bound antibody on the membrane was detected using the SuperSignal West Dura Extended Duration Substrate (Pierce) according to the protocols supplied by the manufacturer. Quantification of bands was performed by using the NIH ImageJ software (available on the World Wide Web at rsb.info.nih.gov/nih-image) following a published method (38).

*Measurement of Proliferation by Using the MTT Assay*—For cell proliferation assays, transfected cells or ganglioside-treated cells, as well as transfection and solvent control cells, respectively, were added to 96-well tissue culture plates at 7000 cells/well in serum-containing medium and cultured for up to 6 days. To quantify cell proliferation, MTT (Sigma) was added to each well (0.5 mg/ml). After incubation for 3.0 h at 37 °C, the supernatants were aspirated, and 100 μl of *n*-propyl alcohol containing 0.1% Nonidet P-40 and 4.0 mM HCl were added. The colorimetric reaction was quantified by using an automatic plate reader, μQuant (Bio-tek Instrument Inc., Winooski, VT) to measure absorbance at 570 nm with a reference filter of 690 nm. Each MTT assay was carried out in triplicate.

*Detection of Apoptosis by Annexin V Flow Cytometry Assays*—The Annexin V/propidium iodide flow cytometry method was used for the detection and quantification of apoptosis in transfected or GD3-treated HEK AD293 cells by following the procedure previously reported for Jurkat cells (39, 40) with the added step of trypsinizing the adherent HEK cells (the previously tested Jurkat cells grow in suspension and did not require this step). After trypsinization and resuspension in complete medium, cells were counted with a Coulter Z2 instrument, and $1.0 \times 10^6$ cells from each sample were pelleted by centrifugation, washed by gentle resuspension in Dulbecco's phosphate-

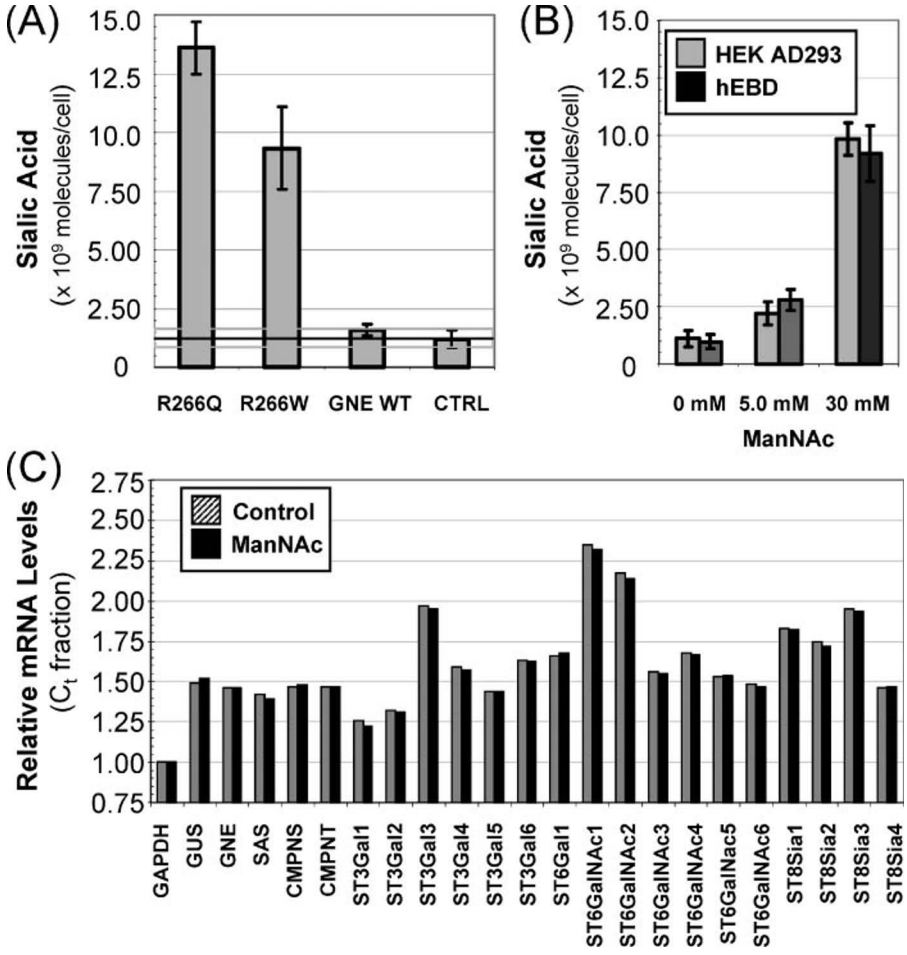


FIGURE 2. **Metabolic flux through the sialic acid pathway and expression of its constituent genes.** *A*, expression of recombinant sialuria (R266Q and R266W) GNEs dramatically increases total sialic acid in HEK AD293 cells, whereas wild-type (*WT*) GNE has a slight (but statistically insignificant, $p > 0.05$) effect. *B*, supplementation of the sialic acid pathway by the addition of ManNAc to the culture medium reproduces the high sialic acid "sialuria" phenotype in HEK AD293 and hEBD LVEC cells. *C*, mRNA levels of sialic acid-processing genes are not altered by the increased flux through the sialic acid pathway that occurs when cells are incubated with ManNAc; qRT-PCR data shown are for hEBD LVEC cells incubated with a 25 mM concentration of this sugar (none of the differences shown are statistically significant with $p \leq 0.05$).

buffered saline, centrifuged again, and suspended in staining buffer. The cells were stained with fluorescein isothiocyanate-labeled Annexin V and propidium iodide and analyzed by flow cytometry as described (39, 40).

*Treatment of Cells with Exogenous Ganglioside GM3 or GD3*—Cells were plated in 6-well tissue culture dishes and incubated until they reached ~60% confluence. GM3 or GD3 (Matreya LLC, Pleasant Gap, PA) was resuspended in serum-free medium and briefly sonicated to ensure appropriate micellar suspension and cellular incorporation of these gangliosides (35, 41, 42). Cells were then incubated in 1.0, 5.0, 10, 20, or 50 $\mu$M GM3 or GD3-containing culture medium in a 37 °C incubator for varying periods of time as indicated throughout. In each case, results were compared with a "solvent control," where an equal volume of medium was added to cells without ganglioside.

## RESULTS

*Overexpression of Recombinant GNE (rGNE) with Sialuria Mutations, but Not Wild-type rGNE, Increases Sialic Acid Production*—Confirmation that perturbations to GNE (with the exception of sialuria mutations) have a minimal impact on sialic acid levels in living cells (due to control exerted over enzyme activity by feedback inhibition) (Fig. 1) was obtained by overexpression of rGNE in HEK AD293 cells. As expected, due to feedback inhibition, sialic acid levels saw only a minimal increase in cells transfected with rGNE compared with the empty vector transfection control samples (Fig. 2*A*). By contrast, expression of rGNE with the R266Q or R266W sialuria mutation that alleviates feedback inhibition (see Fig. 1) resulted in sialic acids levels that were ~7- or ~12-fold higher, respectively (Fig. 2*A*). Previously, similar results were obtained in a Jurkat cell line with an independent set of constructs and transfection conditions (12); these experiments ensured that biologically active GNE was produced under the recombinant expression conditions tested. The confirmation that rGNE had the expected effects on sialic acid production in HEK AD293 cells gave credence to the experiments, described below, probing the nonenzymatic roles of rGNE (*i.e.* the observed catalytic activity of rGNE in supplying metabolic flux into the sialic acid pathway indicated that this protein was properly folded and that it was localized to appropriate parts of the cell to support its normal functions).

*Metabolic Flux through the Sialic Acid Pathway Does Not Alter the Expression of Genes Involved in Sialic Acid Metabolism*—A second set of control experiments was performed to evaluate whether the constituent genes of the sialic acid pathway were responsive to ManNAc or attendant changes in metabolic flux through the pathway. Based on conditions previously established for the Jurkat line (31), exogenously supplied ManNAc was used to supplement sialic acid biosynthesis in the HEK AD293 and hEBD LVEC lines (Fig. 2*B*). By intercepting the sialic acid pathway downstream of the step subject to feedback inhibition, specifically the conversion of UDP-GlcNAc to ManNAc, this strategy allows sialic acid production to increase to levels found in sialuria cells but through a nongenetic mechanism. As previously reported for Jurkat cells (43), none of the genes responsible for sialic acid metabolism listed in Table 1 experienced measurable changes in mRNA levels at ManNAc concentrations up to 30 mM (qRT-PCR results are shown in Fig. 2*C* for the hEBD line incubated with 25 mM ManNAc; similar results were observed for the HEK AD293 line, although fewer sialyltransferases were expressed (data not shown)). Moreover, lower ManNAc concentrations (*e.g.* 0.5 or 1.0 mM) that increase sialic

**TABLE 1**
**Enzymes involved in sialic acid biosynthesis (Fig. 1) and primers used for their analysis by real time PCR**

| Designation[a] | Description/alternative name[b] | Real time PCR primer sequences | |
|---|---|---|---|
| | | Forward primer (5′–3′) | Reverse primer (5′–3′) |
| BiP | UPR chaperone | TAG CGT ATG GTG CTG CTG TC | TTT GTC AGG GGT CTT TCA CC |
| CMPNS | CMP-Neu5Ac synthetase | GCC ATC TTC GAT GGA GT | TAT GTT CAG CTC GCA TTT CG |
| CMPNT | CMP-Neu5Ac transporter | CAA CCA CAG CCG TGT GTA TC | CTG CTG CAT CCA GAT TGC TA |
| GAPDH | (Real time PCR control) | GCA AAT TCC ATG GCA CCG T | TCG CCC CAC TTG ATT TTG G |
| GNE | UDP-GlcNAc 2-epimerase/ManNAc 6-kinase | TGC CCT TCC TAT GAC AAA CTT | GCA TCA CTC GAA CCA TCT CTT |
| GUS | (Real time PCR control) | GAA AAT ATG TGG TTG GAG AGC TCA | CCG AGT GAA GAT CCC CTT TT |
| NCAM | Neural cell adhesion molecule | AAA AGG TGG ATA AGA ACG ACG A | GGT AGA AGT CCT CCA GGT GAT |
| SAS | Sialic acid synthase | CAT GGA TGA GAT GGC AGT TG | GGG GCT TAC CGA TCT GAT AA |
| ST3Gal1 | SIAT4A | ATG TGG ACC CTA TGC TGG AG | CTT GGT CCC AAC ATC AGC TT |
| ST3Gal2 | SIAT4B | AAC CAC CCA CCA TTT CAT GT | TGA TGC TCT GTC CAC CTG TC |
| ST3Gal3 | SIAT6 | TCT AGC TCA CCC CAG GAG AA | GGG ATG CAG GCA TCA GTA AT |
| ST3Gal4 | SIAT4C | CTA GCC ATC ACC AGC TCC TC | GTG GGC AGA TTC AGG GTA GA |
| ST3Gal5 | SIAT9 | CCC TGA ACC AGT TCG ATG TT | CAT TGC TTG AAG CCA GTT GA |
| ST3Gal6 | SIAT10 | TTG CCT CTC TGC TGA GGT TT | CCT CCA TTA CCA ACC ACC AC |
| ST6Gal1 | SIAT1 | GGC ATC AAG TTC AGT GCA GA | TGC GTC ATG ATC ATC GAT TT |
| ST6GalNAc1 | SIAT7A | TCT GGC TGT CCT GGT CTT CT | TGT GTG TTG AGG GCA TTG TT |
| ST6GalNAc2 | SIAT7B | ACC AGA AGC CTC TGC CAG TA | ATG GCT TCA TTT TTC GTT CG |
| ST6GalNAc3 | SIAT7C | CCA GAA GGT GGG AAA TGA GA | TTC CTC ATA TTG CGG AAA GG |
| ST6GalNAc4 | SIAT3C | CTG CAG CTC ACC AGG ATG TA | TCC CAT AGA CCA CGA TCT CC |
| ST6GalNAc5 | SIAT7E | TTA CTC GCC ACA AGA TGC TG | GCA CCA TGC CAT AAA CAT TG |
| ST6GalNAc6 | SIAT7F | CTC CGG AGA GAA ATG AGT AG | CAG TGT CTT GTT GCC GAG AA |
| ST8Sia1 | SIAT8A | AGC GTT CAG GAA ACA AAT GG | TGC CTG TGG GAA GAG AGA GT |
| ST8Sia2 | SIAT8B | TGA CCA ACA AAG TCC ACA TCA | TGG GAG GTG TAG CCA TAC TTG |
| ST8Sia3 | SIAT8C | TCC CTG CAT TTT TCT TCC AC | ACG GCC AAA ATC CAT ACA AG |
| ST8Sia4 | SIAT8D | ACG GCC AAA ATC CAT ACA AG | CTT AGG GAA GGG CCA GAA TC |

[a] Sialyltransferase nomenclature as designated by the Human Genome Organization (HUGO) is given in this column; the HUGO nomenclature (ST3Gal5 and ST8Sia1) is used throughout for the GM3 and GD3 synthases, respectively.
[b] The outdated, but still occasionally used, "SIAT*n*" sialyltransferase nomenclature is provided in the second column.

acid levels marginally (similar to levels observed after transfection with wild-type rGNE) (Fig. 2*A*) likewise did not lead to changes in mRNA levels for any of the sialic acid processing genes (data not shown). The lack of "ManNAc-responsive" genes confirmed that the gene expression changes subsequently discussed in this paper were not simply the result of changes in metabolic flux through the sialic acid pathway or the simple presence of ManNAc.

*Overexpression and RNAi Knock Down of GNE Change ST3Gal5 and ST8Sia1 mRNA Levels*—The transfection of wild-type rGNE into HEK AD293 cells resulted in a ~10-fold increase in GNE mRNA compared with empty vector transfection controls (Fig. 3*A*). In the same cells, the levels of ST3Gal5 and ST8Sia1 sialyltransferase mRNAs also showed a statistically significant, although smaller, increase of ~50% (Fig. 3*A*); by contrast, the expression of other sialyltransferases (listed in Table 1 and shown in Fig. 2*C*) was not measurably changed (data not shown).

Next, to test whether the opposite response in ST3Gal5 and ST8Sia1 expression would occur upon a decrease in GNE, RNAi methods were used to reduce GNE expression. First, three short hairpin RNA (shRNA) sequences (44, 45) were evaluated (shGNE760, shGNE827, and shGNE1448) in HEK AD293 cells and each led to a significant decrease in mRNA levels of GNE compared with the transfection control (Fig. 3*B*). To verify the specificity of shRNAs for GNE, the shGNE760 sequence, which was the most effective of the three constructs at reducing GNE mRNA levels, was evaluated by a second RNAi method, siRNA (44). In this experiment, the ability of double-stranded small interfering GNE760 RNA to reduce GNE mRNA to the same levels as the shGNE760 construct (Fig. 3*B*) verified that these effects were sequence-specific and were unlikely to be due to off-target gene regulation that can occur in RNAi experiments (46). In the next experiment, a quantitative analysis of ST3Gal5 and ST8Sia1 mRNA in cells transfected with shGNE760 showed a significant decrease for both of these sialyltransferases compared with the transfection controls (Fig. 3*C*). Together with the rGNE results presented earlier, these RNAi experiments provide consistent evidence of a correlation between GNE mRNA levels and the expression of the ST3Gal5 and ST8Sia1 sialyltransferases.

*Up- or Down-regulation of GNE Changes GM3 and GD3 Levels Correspondingly*—Next, we measured GM3 and GD3 to ensure that changes in ST3Gal5 and ST8Sia1 mRNA levels, as reported above, were reflected in the actual cellular levels of the ganglioside produced by each enzyme. As shown in Fig. 4, GM3 and GD3 levels were higher in cells where rGNE was overexpressed compared with empty vector transfection controls (Fig. 4*A*), a result consistent with the increased mRNA levels of ST3Gal5 and ST8Sia1 in these cells. Conversely, levels of GM3 and GD3 were lower in cells where GNE was down-regulated by shRNAs and siRNAs (representative data for shGNE760 are shown in Fig. 4*B*, and the summation of several replicates is shown in Fig. 4*C*), consistent with the lower levels of ST3Gal5 and ST8Sia1 in these cells. Because GD3 levels have not been previously reported for HEK AD293 cells, SK-MEL-28 cells, which have very high levels of this ganglioside (28, 47), were analyzed to provide a benchmark for GD3 levels in the HEK line. For comparison, the HEK cells were found to have ~10% of the GD3 present in the SK-MEL-28 line (data not shown).

On a technical note, the amount of GM3 produced by ST3Gal5 may have been underestimated in this work, because this ganglioside can be converted to GM2 by GalGT and subsequently to GM1 by B3GalT4 (as outlined in Fig. 3*D*; quantification of GM1 and GM2 was beyond the scope of the current report). Similarly, GD3 produced by the up-regulation of

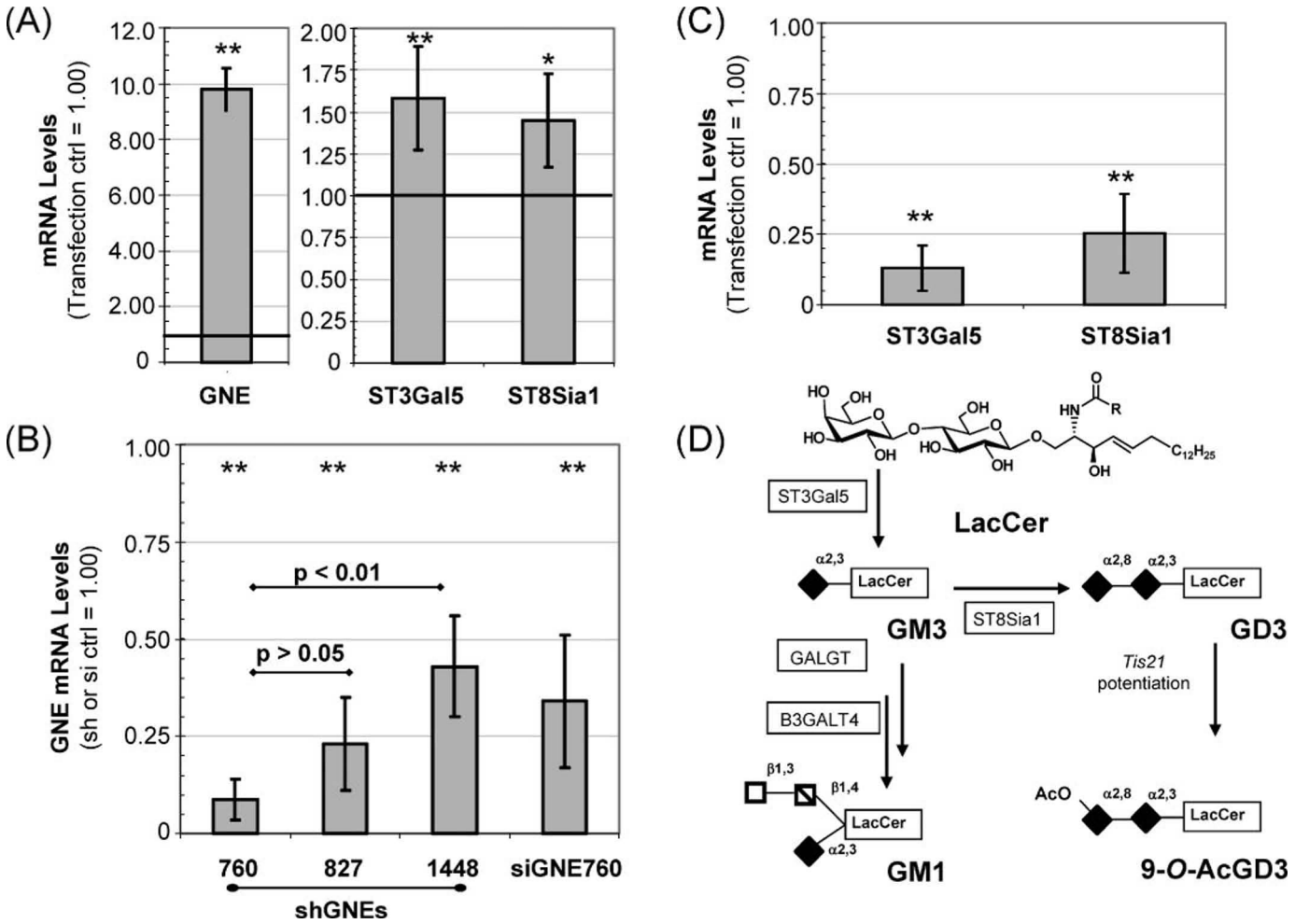


FIGURE 3. **Effects of overexpression or inhibition of GNE.** *A*, overexpression of rGNE increases GNE, ST3Gal5, and ST8Sia1 mRNA levels as determined by qRT-PCR in HEK AD293 cells transfected with wild-type GNE (values are compared with the empty vector transfection control arbitrarily set at 1.00). *B*, expression of GNE mRNA in cells treated with shRNA or siRNA (values are relative to control transfections where expression was normalized to 1.00). *C*, ST3Gal5 and ST8Sia1 mRNA levels in cells treated with shGNE760 (from *B*). *D*, ST3Gal5 and ST8Sia1 sequentially convert LacCer to gangliosides GM3 and GD3, respectively. GM3 can be further converted to other gangliosides, such as GM1 not analyzed in this study, and GD3 and be acetylated at the 9-position of the terminal sialic acid (*, $p \leq 0.05$; **, $p \leq 0.01$; each data point represents a minimum of three replicates).

ST8Sia1 can undergo further modification by 9-*O*-acetylation (see the chemical structures in Fig. 1). In this case, however, the antibody used for GD3 detection was deliberately selected because it recognized both forms of GD3, allowing the aggregate level of both forms of this ganglioside to be estimated. Notwithstanding the need for additional studies to fully characterize the metabolic connections between gangliosides and GNE, the information currently in hand is sufficient to verify that the effects of GNE on the mRNA levels of ST3Gal5 and ST8Sia1 translate into the corresponding phenotypic changes (*i.e.* changes to GM3 and GD3 levels) in cells.

*Verification of the Flow Cytometry Detection Method by Analysis of the Uptake of Exogenous Gangliosides*—In many studies, gangliosides have been evaluated after extraction from cells by organic solvents followed by separation and detection by TLC. There are several limitations to this approach that posed difficulties in the present study. These challenges included small changes in GM3 and GD3 levels in rGNE-transfected cells (see Fig. 4) that could not be accurately quantified by TLC analysis; the large number of cells required for ganglioside extraction exceeded the capacity of reproducible transfection protocols, and the subcellular distribution of the gangliosides could not be determined by TLC. Therefore, we used flow cytometry, a method capable of detecting small shifts in cellular distributions of gangliosides such as GD3 (28, 35, 47–50) in this study. However, to address concerns raised by reports that work-up conditions alter cellular and tissue distributions of gangliosides (51) and to ensure that the flow cytometry method provided biologically-relevant results in our hands, we tested the concentration and time dependence of the uptake of endogenous GM3 and GD3. In these tests, we observed ganglioside uptake and incorporation consistent with literature reports (52). Specifically, time- and dose-dependent increases in GM3 (Fig. 5) and GD3 (Fig. 6) occurred with the anticipated kinetics (*i.e.* a 30 min time point gave distinct results compared with time periods of greater than 2.0 h) and over the expected concentrations ($\leq$100 $\mu$M).

A second purpose for the characterization of ganglioside uptake by flow cytometry was to verify the mechanism of cellular uptake and incorporation of exogenous GM3 and GD3 and their subsequent ability to function as endogenous gangliosides (35, 41). These experiments could provide evidence, albeit indi-

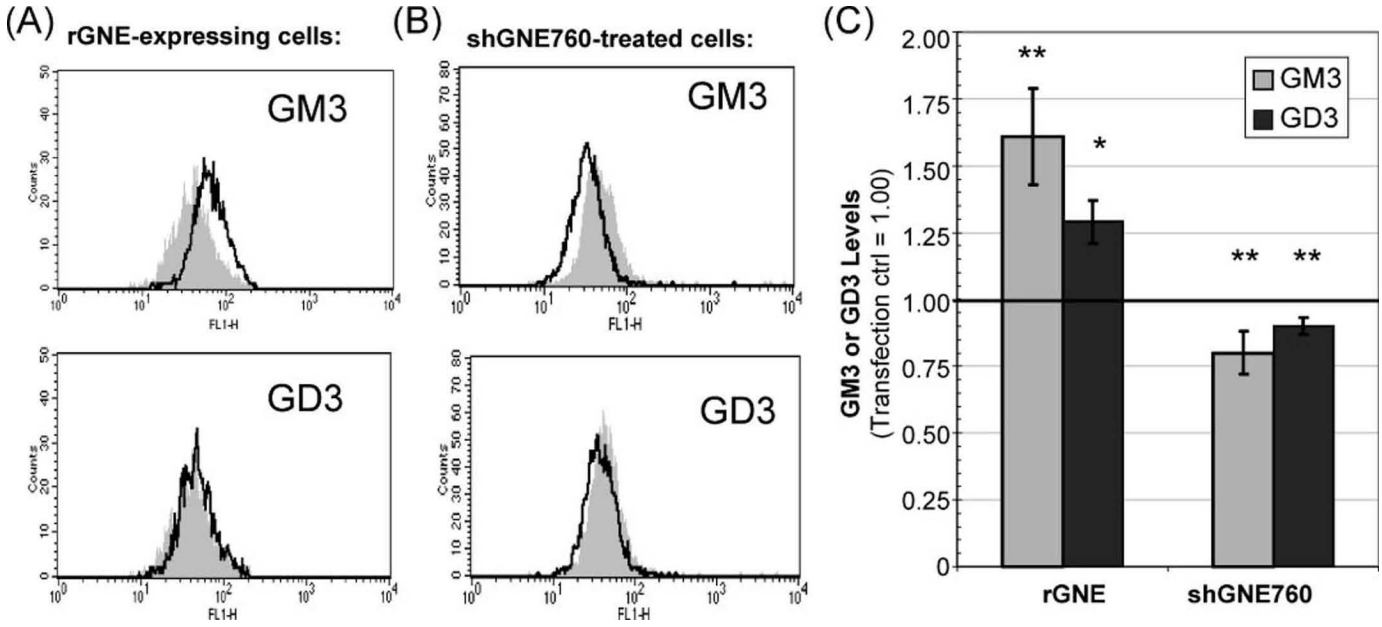


FIGURE 4. **rGNE-induced changes in ST3Gal5 and ST8Sia1 expression result in corresponding changes to GM3 and GD3 levels.** HEK AD293 cells overexpressing rGNE experienced increased levels of GM3 and GD3 (*A*), whereas cells exposed to siRNAs experienced reduced levels of these gangliosides, as shown by representative flow cytometry histograms (the transfection control is shown in *solid gray*, and the data for rGNE- or shGNE760-treated cells are shown in the *black outline* format) (*B*). *C*, flow cytometry data from a minimum of three replicates is pooled for the rGNE and shGNE760 samples (*, $p \leq 0.05$; **, $p \leq 0.01$). In this figure and throughout this report, the antibody used to detect GD3 also recognizes the 9-*O*-acetyl form of GD3.

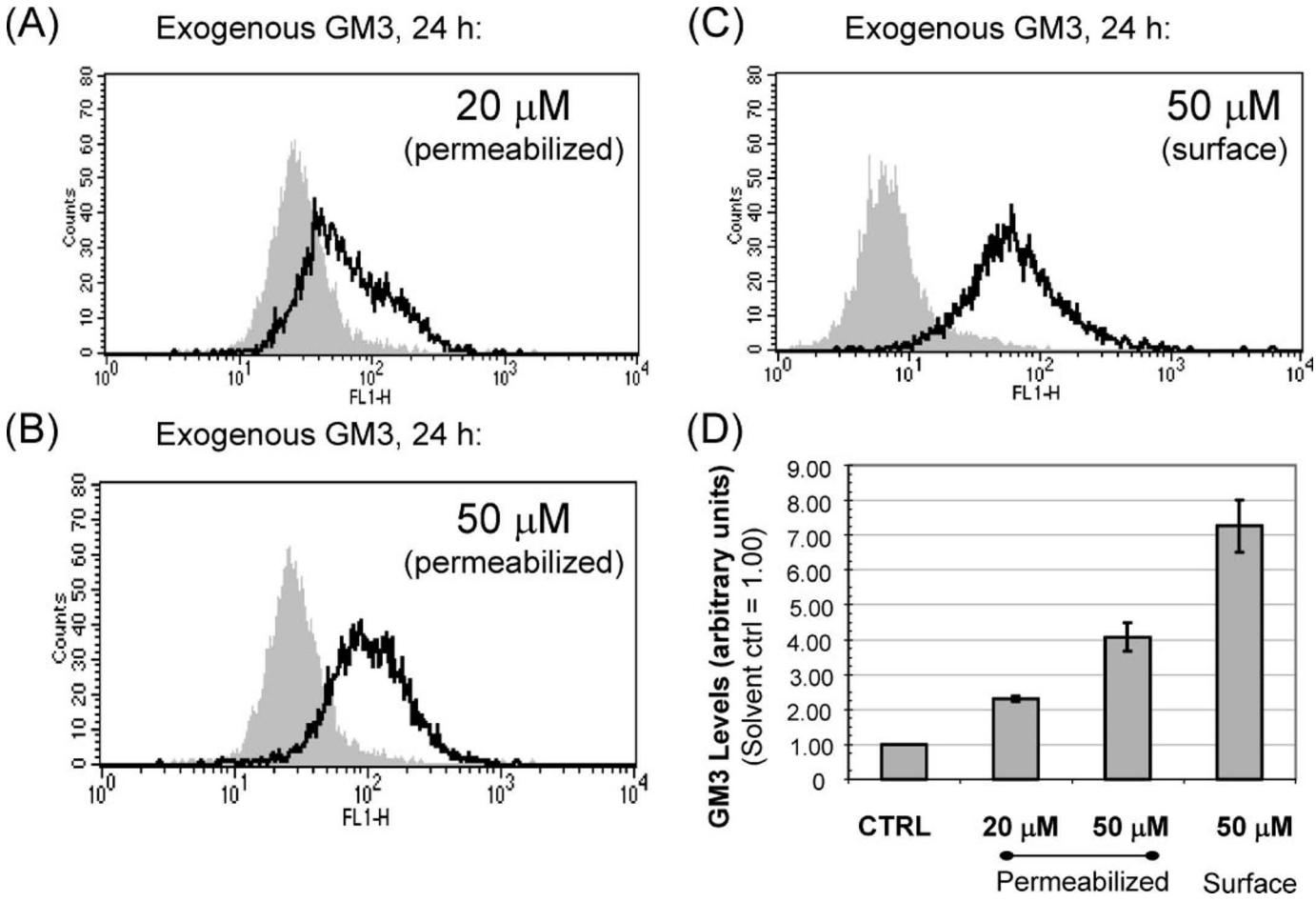


FIGURE 5. **Measurement of GM3 levels by flow cytometry in HEK AD293 cells exposed to exogenous ganglioside.** Representative flow cytometry data are shown for GM3 in permeabilized cells exposed to 20 $\mu$M (*A*) or 50 $\mu$M (*B*) GM3 as well as for intact cells exposed to 50 $\mu$M GM3 (*C*). In these plots, data for "solvent" control cells are shown in *solid gray*, and the data for GM3-exposed cells are shown in *black outline*. *D*, quantified fluorescence levels from flow cytometry data are summarized for a minimum of three replicates. *, $p \leq 0.05$; **, $p \leq 0.01$.

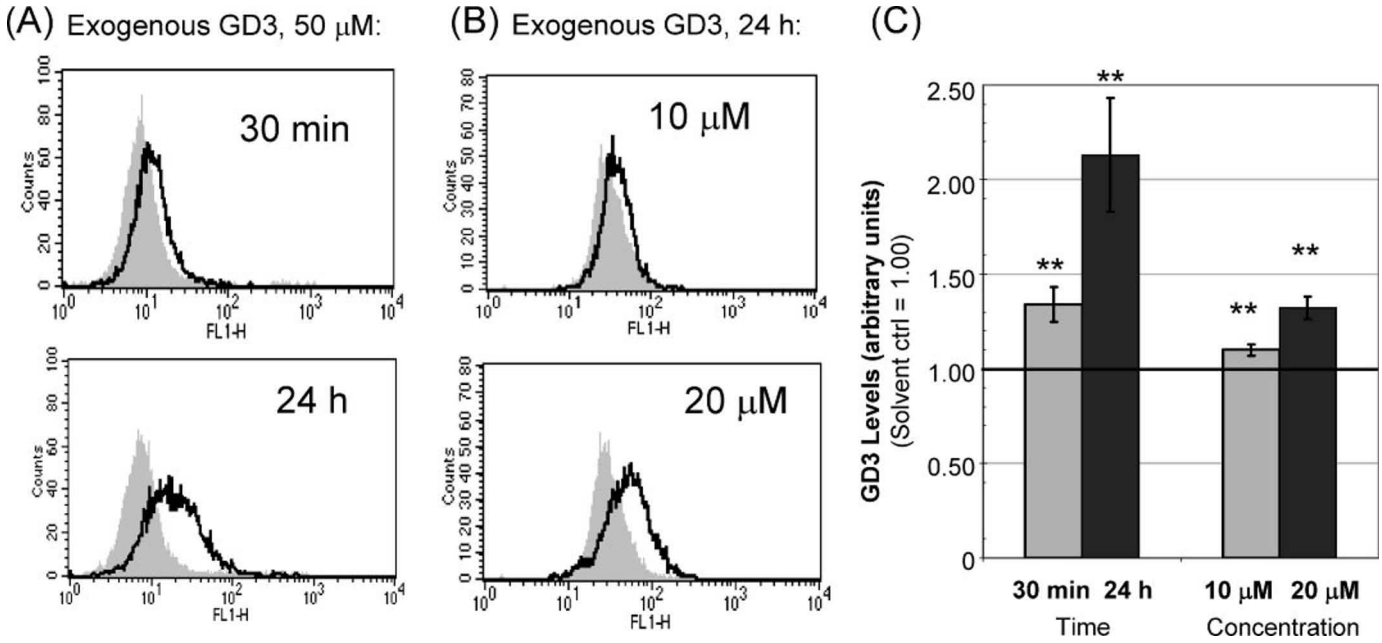


FIGURE 6. **Measurement of GD3 levels by flow cytometry in HEK AD293 cells exposed to exogenous ganglioside.** GD3 uptake is both time-dependent (*A*) and concentration-dependent (*B*), as shown by representative flow cytometry results (data for "solvent" control cells are shown in *solid gray*, and the data for GM3-exposed cells are shown in *black outline*). *C*, data are summarized for a minimum of three replicates. *, $p \leq 0.05$; **, $p \leq 0.01$.

rectly, that the cellular responses mediated by GNE were elicited through gangliosides, because, if exogenous GM3 or GD3 did not lead to similar cellular responses (in apoptosis and proliferation, as described in more detail below) as GNE-mediated up-regulation of ST3Gal5 and ST8Sia1, these gangliosides could be eliminated as intermediaries of these effects. After initial association with a cell, gangliosides translocate from the plasma membrane to intracellular compartments, such as the mitochondria or Golgi, for their full effects on apoptosis or proliferation to be realized. Consequently, it was reassuring that cells exposed to 50 μM GM3, given sufficient time (24 h) to allow ganglioside internalization and then fixed and permeabilized to allow intracellular compartments to be stained, showed higher levels of this ganglioside (Fig. 5*A*) compared with intact cells, where only surface gangliosides were stained (Fig. 5*B*). Moreover, the relative difference between the treated and control cells was greater for surface staining than for permeabilized cells (Fig. 5*C*); this result was consistent with reports that describe the rapid uptake of GM3 into the plasma membrane (52), followed by slower trafficking to internal organelles (41). As a caveat, these comparisons must be regarded with caution due to the possible ganglioside relocations or increased accessibility that may have occurred due to the fixing process (51), but, at a minimum, they do not raise any red flags to discount the biological processing or detection methodology used in this study.

*GNE mRNA Levels Modulate Apoptosis and Proliferation*—Based on reports that GM3 and GD3 have an impact on apoptosis and proliferation (53–56), combined with the connections between GNE and these gangliosides uncovered in this study, we tested these two parameters in cells overexpressing rGNE and in cells treated with shGNE760 to reduce GNE expression. The overexpression of rGNE resulted in a moderate increase in apoptotic cells (Fig. 7*A*) compared with empty vector transfection controls (Fig. 7*B*; the transfection process itself increased apoptotic cells from ~4–7% seen under normal culture conditions to ~20% (data not shown)). As expected for cells under apoptotic stress, proliferation decreased upon transfection of rGNE. By contrast, proliferation increased in cells transfected with shGNE760 (Fig. 7*C*), a procedure that led to reduced levels of mRNA for GNE. Together, these two results establish an inverse correlation between GNE levels and cell growth rates in HEK AD293 cells.

*Exogenously Supplied GM3 and GD3 Influence Proliferation*—The results reported above establish a chain of events where GNE regulates sialyltransferase expression, which in turn modulates levels of GM3 and GD3 that, finally, have an impact on cell growth. To support this hypothesis, where downstream effects of GNE are mediated through GM3 and GD3 (57), HEK AD293 cells were exposed to these gangliosides and monitored by the MTT assay. In these experiments, GM3 inhibited proliferation over the 1.0–50 μM concentration range, with data shown for 5.0 and 10 μM (Fig. 7*D*); GD3 was also inhibitory at 10 μM. These results are consistent with a mechanism of action of GNE, where it increases the production of GM3 and GD3 (Figs. 3 and 4), which in turn inhibit proliferation (Fig. 7*C*). Interestingly, GD3 had the opposite effect at 5.0 μM and stimulated proliferation (Fig. 7*D*); although beyond the scope of the current investigation, resolving the concentration-dependent effects of GD3 will probably require careful analysis of conversion of this ganglioside to 9-*O*-AcGD3 (Fig. 3*D*). Of particular relevance to the current results, GD3 is a potent inducer of apoptosis, whereas 9-*O*-AcGD3 has antiapoptotic properties (55, 58). Consequently, if the acetylation mechanism that was recently reported to be activated by GD3 exposure (35) and provides a protective, proproliferative response at low levels (*e.g.* at 5.0 μM) (Fig. 7*D*) becomes overwhelmed at higher levels of exposure, the proapoptotic, antiproliferative effects

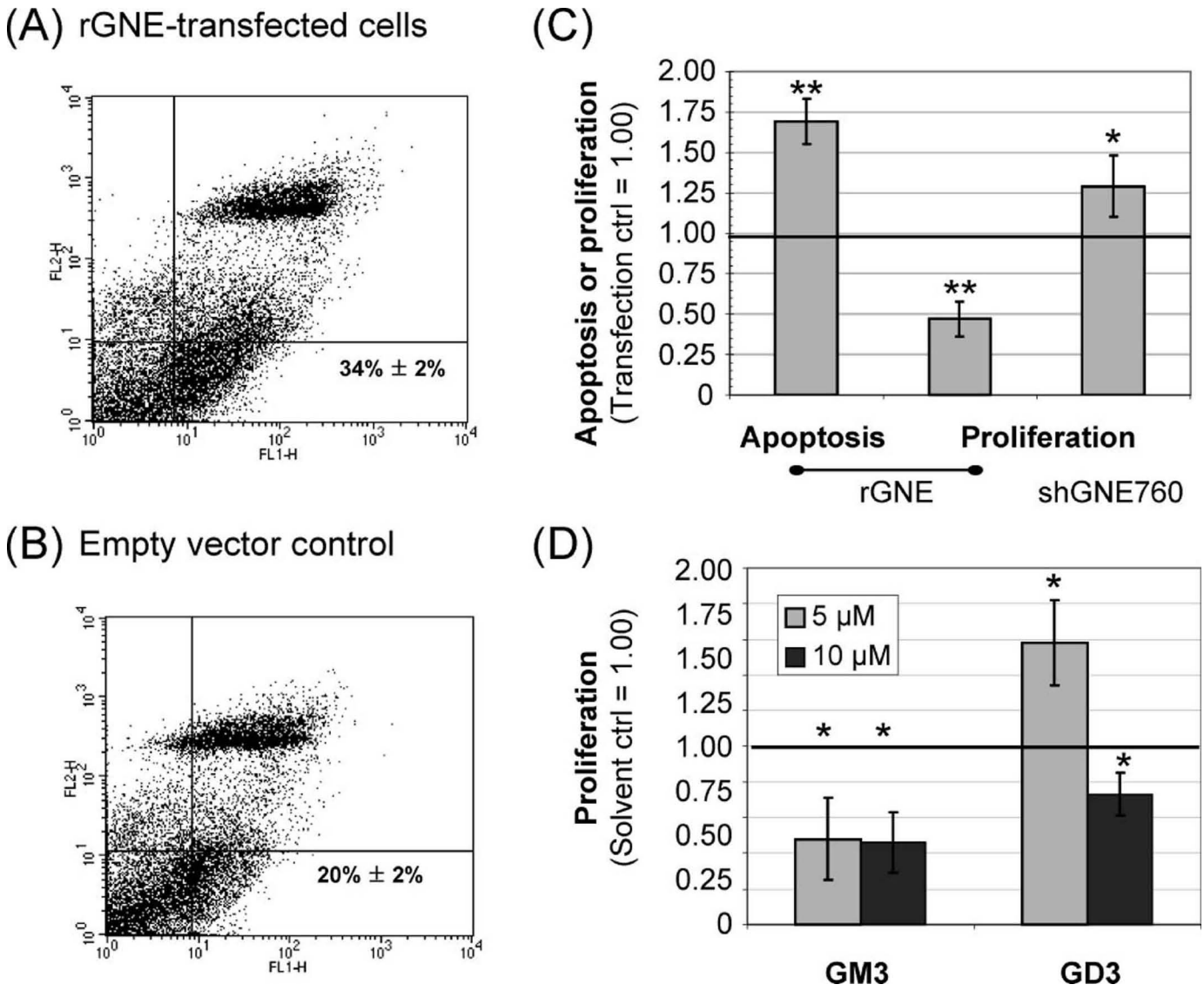


FIGURE 7. **Apoptosis and proliferation is controlled by GNE and gangliosides GM3 and GD3 in HEK AD293 cells.** Apoptosis increased in rGNE-transfected cells (*A*) compared with empty vector (*EV*) controls (*B*) in annexin V flow cytometry assays. *C*, apoptosis, determined from a minimum of three replicates (see *A* and *B*) and proliferation, determined from MTT assays, are shown for cells transfected with rGNE or shGNE760. *D*, proliferation in cells exposed to exogenous GM3 and GD3 determined from MTT assays. *, $p \leq 0.05$; **, $p \leq 0.01$ (*C* and *D*).

of the unmodified form of GD3 would be manifest (*e.g.* at 10 $\mu$M) (Fig. 7*D*).

*Exogenous Gangliosides Regulate GNE and BiP mRNA Levels*—GM3 and GD3, the two gangliosides whose production was influenced by GNE (Fig. 3), have been reported to regulate gene expression; to give one example, GD3 selectively induces transcription and new protein synthesis required for 9-*O*-acetylation of itself (35). Results from the current experiments extend the genes regulated by these gangliosides to include GNE and BiP (Fig. 8, *A* and *B*). Gene regulation via these gangliosides is highly specific, as shown by the reduction in GNE mRNA at all concentrations of GM3 tested (10 $\mu$M is shown in Fig. 8*A*) as well as at higher (*e.g.* $\geq$10 $\mu$M) levels of GD3 (Fig. 8*A*). Interestingly, consistent with the results described above, where the effects of GD3 on proliferation were concentration-dependent, GD3 at relatively low levels (*e.g.* $\leq$5.0 $\mu$M) had the opposite effect of stimulating GNE mRNA production. Conversely, levels of BiP mRNA were higher under the three conditions that led to decreased levels of GNE mRNA (*e.g.* GM3 at 5.0 and 10 $\mu$M and GD3 at 10 $\mu$M) and was lower at the concentration of GD3 (*i.e.* $\leq$5.0 $\mu$M) that had led to increased levels of GNE mRNA.

*Modulation of Proliferation by GNE and Gangliosides Occurs via ERK1/2 Phosphorylation*—Based on the connections between GNE, gangliosides, and proliferation presented in this paper, combined with several reports implicating GM3 (59) and GD3 (60, 61) in the regulation of cell proliferation via MAPK signaling pathways, we analyzed the phosphorylation of ERK1/2 by Western analysis (Fig. 9). In the current experiments, ERK1/2 levels were not noticeably affected by any treatment. By contrast, rGNE expression, which led to increased GD3 levels (Fig. 4*C*), resulted in an increased level of phosphorylation of ERK1/2, as did the direct supplementation of cells with GD3 (Fig. 9*A*). Conversely, the knock down of GNE by shGNE670 had the opposite effect, with lower phosphorylation of ERK1/2 compared with the transfection control. Together,

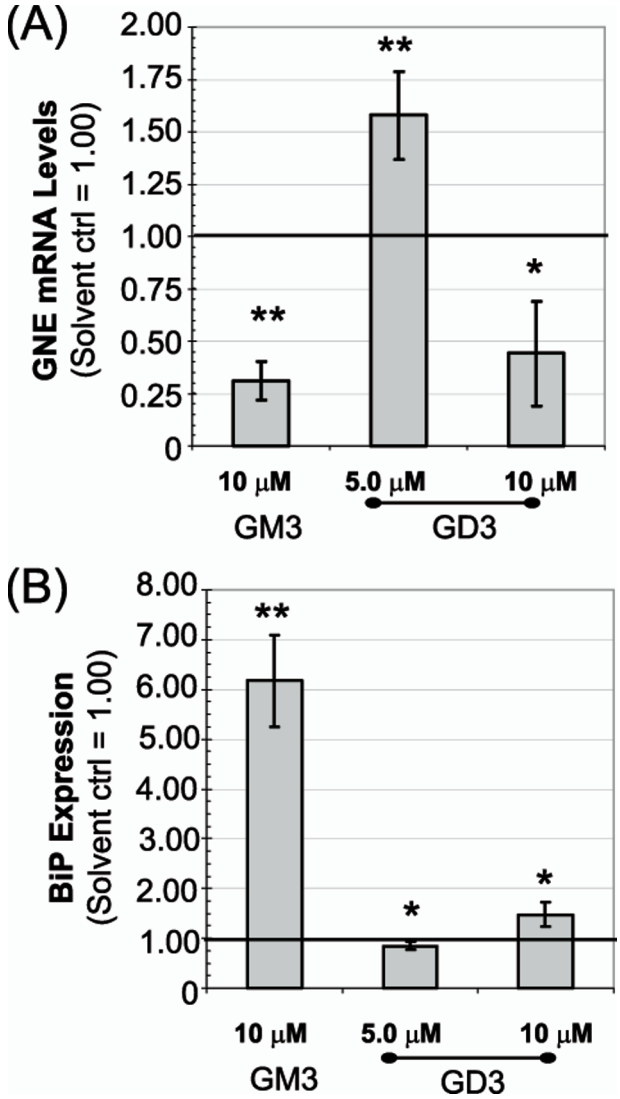


FIGURE 8. **GM3 and GD3 regulate the expression of GNE and BiP.** Exogenous GM3 and GD3 alter GNE (*A*) and BiP (*B*) mRNA levels. mRNA levels for GNE and BiP were determined in triplicate by real-time PCR after exposure of HEK AD293 cells to GM3 or GD3 (*, $p \leq 0.05$; **, $p \leq 0.01$).

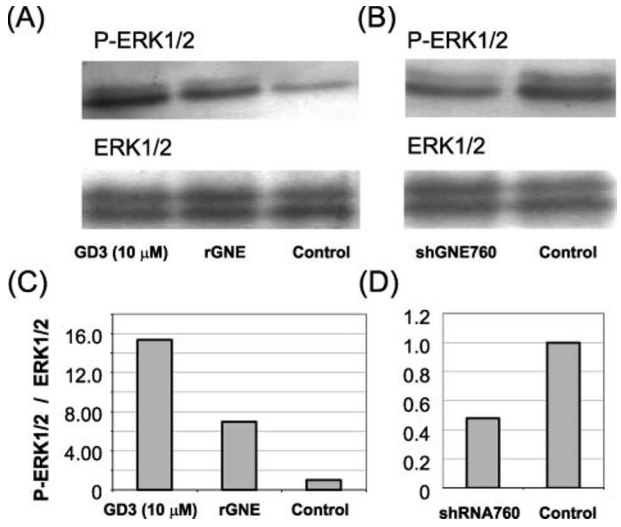


FIGURE 9. **Western analysis of ERK1/2 and phosphorylated ERK1/2 (*P-ERK1/2*).** *A*, exogenous GD3 (at 10 μM) or rGNE expression increases phospho-ERK1/2 compared with untreated controls (*top*) without causing a noticeable change in total ERK1/2 (*bottom*). *B*, conversely, shGNE760 decreases P-ERK1/2, consistent with the knock down of GNE (see Fig. 4*C*). Note that the exposure conditions were different in *A* and *B* so that a direct quantitative comparison cannot be made between these panels. Densitometry, therefore, was used to normalize data for each panel by arbitrarily setting the phospho-ERK1/2 to ERK1/2 ratio at 1 for control samples and adjusting the test samples accordingly (*C* and *D*).

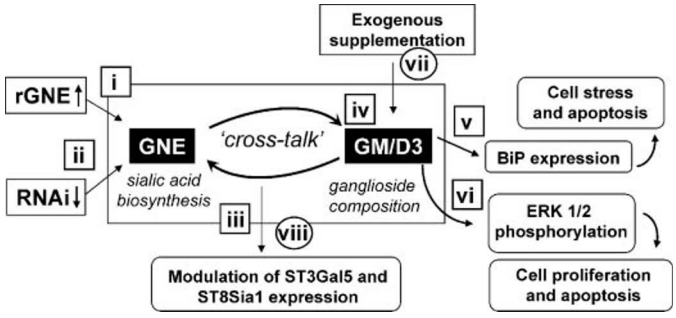


FIGURE 10. **Connections between GNE, sialic acid metabolism, gangliosides, and "downstream" cellular responses.** The two methods (rGNE (*i*) and shRNA (*ii*)) that were used to perturb GNE mRNA levels expression led to changes in ST3Gal5 and ST8Sia1 mRNA (*iii*) as well as to the levels of the corresponding gangliosides GM3 and GD3 (*iv*). These gangliosides then produced changes in cellular behavior including increased apoptosis through BiP expression (*v*) and cell proliferation through ERK1/2 phosphorylation (*vi*). Incorporation of exogenous gangliosides (*vii*) led to the same responses in BiP and ERK1/2 and, interestingly, also had the "upstream" effect of altering ST3Gal5 and ST8Sia1 expression (*viii*), leading us to hypothesize that two-way cross-talk occurs between GNE and gangliosides.

the rGNE transfection experiments, the exogenous supplementation of cells with GD3, and the shRNA data provide a consistent picture where GNE expression and subsequent changes to GD3 levels are positively correlated with ERK1/2 phosphorylation (Fig. 9) and attendant changes in proliferation (Fig. 8).

## DISCUSSION

Over the past decade, the conversion of UDP-GlcNAc to ManNAc and the subsequent phosphorylation of the latter compound by GNE have been studied extensively (6, 62). Now, based on accumulating evidence that this protein has additional functions beyond producing metabolites needed for sialic acid biosynthesis, we have identified an expanded repertoire of activities for GNE. In these experiments, which are summarized in Fig. 10, we first used a complementary pair of methods to up- and down-regulate GNE expression and observed corresponding changes to mRNA levels of ST3Gal5 and ST8Sia1 (Fig. 3) as well as in the production of the gangliosides, GM3 and GD3, made by these sialyltransferases (Figs. 4 and 5). Multifaceted bioactivities have been reported for GM3 and GD3, including regulation of senescence, apoptosis, proliferation, and migration (63, 64). As a result, GNE-initiated changes in the production of these gangliosides have the potential to elicit wide-ranging changes in cellular physiology.

In this report, we focused on the influence that GM3 and GD3 exert over apoptosis and proliferation by demonstrating the involvement of these versatile molecules in biochemical pathways that regulate both of these processes. First, based on a report connecting gangliosides to BiP (65), a protein involved in activation of the unfolded protein response and associated apoptosis (66, 67), we found that GM3 and GD3 regulated BiP mRNA levels (Fig. 8). Then, based on several reports implicating GM3 (59) and GD3 (60, 61) in the regulation of cell prolif-

eration via MAPK signaling pathways, we showed that GNE-mediated changes to proliferation occurred through phosphorylation of ERK1/2 (Fig. 9). This response typifies biochemical signaling pathways that operate via rapid phosphorylation cascades in contrast to other GNE-mediated responses that required mRNA production and (presumably) *de novo* protein and glycolipid synthesis. Together, by exerting control over cellular processes by multiple mechanisms, GNE is proving to be a central player in cell biology.

Control experiments, where exogenous ManNAc was used to mimic the effects of rGNE on sialic acid metabolism by increasing flux into the biosynthetic pathway, were included in this study and are important for two reasons. First, it was necessary to determine if a suite of "ManNAc-responsive" genes, analogous to the set of genes regulated by glucose (68), exist. It also was important to test whether the rate of flux of the metabolic intermediate CMP-Neu5Ac through the nucleus influences gene expression, a possibility that arose from suggestions that CMP-Neu5Prop, a nonnatural derivative of CMP-Neu5Ac, had such an effect (69). The lack of a metabolic flux-specific response (Fig. 2*C*) ensured that the "downstream" effects of GNE on sialyltransferase expression, ganglioside production, and proliferation were not just an extremely subtle (and therefore previously undetected) consequence of the primary role of this protein in controlling sialic acid biosynthesis.

Once sialic acid production was discounted as the mechanism by which GNE controlled sialyltransferase expression, ganglioside production, and the subsequent modulation of proliferation and apoptosis, the next step was to uncover the underlying mechanisms that mediate noncanonical GNE responses. Although an experimental investigation of mechanism is beyond the scope of this report, a sufficient scientific foundation is in place to develop a working model to guide future investigations. To elaborate briefly, the GNE-mediated response can be divided into two distinct segments that probably utilize unique biochemical mechanisms. The first activity, the forward direction "cross-talk" (as shown in Fig. 10) that links GNE with sialyltransferase expression and GM3 and GD3 levels, is far from understood. Notwithstanding the current lack of experimental support for the following hypothesis, a recent report that GNE shuttles to the nucleus (27), where its enzymatic activities are not required, makes it tempting to speculate that GNE plays a role in transcription either directly or by associating with transcription factors.

Following GNE-initiated changes to cellular levels of GM3 and GD3, a second sequence of events unfolds that is conceptually well understood and can be invoked to explain how these gangliosides influence gene expression. To recap, the set of genes underwent regulation by gangliosides, including BiP in the "downstream" direction and GNE in the "upstream" direction (Fig. 8). A scenario to explain these results is based on the clustering of gangliosides into microdomains, termed "glycosynapses" (70). These assemblies participate in carbohydrate-dependent cell adhesion, and they concurrently modulate signal transduction and influence cellular phenotypes (71, 72) by ultimately regulating the expression of numerous genes. Of particular relevance to the current work, GM3 has been reported to be an important component of the glycosynapses (73) that modulate MAPK pathways (48, 74), thereby offering an explanation for the effects of gangliosides on ERK1/2 phosphorylation shown in Fig. 9.

In conclusion, the ability of GM3 and GD3 to influence GNE mRNA levels, probably through complex signal transduction pathways modulated through glycosynapse microdomain assemblies, represents a new feedback control mechanism for this protein that supplements the previously described epigenetic regulation of GNE gene expression through methylation (62). In turn, these two mechanisms complement allosteric feedback inhibition, where CMP-Neu5Ac binding inhibits the enzymatic activity of GNE (Fig. 1). Considering the several critical cellular functions of GNE, which include control over sialic acid production as well as the life and death of a cell, it is not surprising that GNE is carefully regulated with multiple layers of control.

*Acknowledgment—We are grateful to K. Konstantopoulos for flow cytometer access.*

## REFERENCES


1. Schauer, R. (2004) *Arch. Biochem. Biophys.* **426,** 132–141
2. Angata, K., and Fukuda, M. (2003) *Biochimie* (*Paris*) **85,** 195–206
3. Varki, A. (1997) *FASEB J.* **11,** 248–255
4. Tanner, M. E. (2005) *Bioorg. Chem.* **33,** 216–228
5. Hinderlich, S., Stäche, R., Zeitler, R., and Reutter, W. (1997) *J. Biol. Chem.* **272,** 24313–24318
6. Keppler, O. T., Hinderlich, S., Langner, J., Schwartz-Albiez, R., Reutter, W., and Pawlita, M. (1999) *Science* **284,** 1372–1376
7. Jeffery, C. J. (2003) *Trends Genet.* **19,** 415–417
8. Copley, S. D. (2003) *Curr. Opin. Chem. Biol.* **7,** 265–272
9. Seppala, R., Lehto, V. P., and Gahl, W. A. (1999) *Am. J. Hum. Genet.* **64,** 1563–1569
10. Weiss, P., Tietze, F., Gahl, W. A., Seppala, R., and Ashwell, G. (1989) *J. Biol. Chem.* **264,** 17635–17636
11. Seppala, R., Tietze, F., Krasnewich, D., Weiss, P., Ashwell, G., Barsh, G., Thomas, G. H., Packman, S., and Gahl, W. A. (1991) *J. Biol. Chem.* **266,** 7456–7461
12. Yarema, K. J., Goon, S., and Bertozzi, C. R. (2001) *Nat. Biotechnol.* **19,** 553–558
13. Chen, H., Wang, Z., Sun, Z., Kim, E. J., and Yarema, K. J. (2005) in *Handbook of Carbohydrate Engineering* (Yarema, K. J., ed) pp. 1–48, Francis & Taylor/CRC Press, Inc., Boca Raton, FL
14. Zachara, N. E., and Hart, G. W. (2002) *Chem. Rev.* **102,** 431–438
15. Hanover, J. A. (2001) *FASEB J.* **15,** 1865–1876
16. Watts, G. D. J., Thorne, M., Kovach, M. J., Pestronk, A., and Kimonis, V. E. (2003) *Neuromuscul. Disord.* **13,** 559–567
17. Tomimitsu, H., Shimizu, J., Ishikawa, K., Ohkoshi, N., Kanazawa, I., and Mizusawa, H. (2004) *Neurology* **62,** 1607–1610
18. Eisenberg, I., Thiel, C., Levi, T., Tiram, E., Argov, Z., Sadeh, M., Jackson, C. L., Thierfelder, L., and Mitrani-Rosenbaum, S. (1999) *Genomics* **55,** 43–48
19. Eisenberg, I., Avidan, N., Potikha, T., Hochner, H., Chen, M., Olender, T., Barash, M., Shemesh, M., Sadeh, M., Grabov-Nardin, G., Shmilevich, I., Friedmann, A., Karpati, G., Bradley, W. G., Baumbach, L., Lancet, D., Ben Asher, E., Beckmann, J. S., Argov, Z., and Mitrani-Rosenbaum, S. (2001) *Nat. Genet.* **29,** 83–87
20. Penner, J., Mantey, L. R., Elgavish, S., Ghaderi, D., Cirak, S., Berger, M., Krause, S., Lucka, L., Voit, T., Mitrani-Rosenbaum, S., and Hinderlich, S. (2006) *Biochemistry* **45,** 2968–2977
21. Nishino, I., Noguchi, S., Murayama, K., Driss, A., Sugie, K., Oya, Y., Nagata, T., Chida, K., Takahashi, T., Takusa, Y., Ohi, T., Nishimiya, J., Sunohara, N., Ciafaloni, E., Kawai, M., Aoki, M., and Nonaka, I. (2002) *Neurol-*

*ogy* **59,** 1689–1693
22. Noguchi, S., Keira, Y., Murayama, K., Ogawa, M., Fujita, M., Kawahara, G., Oya, Y., Imazawa, M., Goto, Y., Hayashi, Y. K., Nonaka, I., and Nishino, I. (2004) *J. Biol. Chem.* **279,** 11402–11407
23. Hinderlich, S., Salama, I., Eisenberg, I., Potikha, T., Mantey, L. R., Yarema, K. J., Horstkorte, R., Argov, Z., Sadeh, M., Reutter, W., and Mitrani-Rosenbaum, S. (2004) *FEBS Lett.* **566,** 105–109
24. Salama, I., Hinderlich, S., Shlomai, Z., Eisenberg, I., Krause, S., Yarema, K. J., Argov, Z., Lochmuller, H., Reutter, W., Dabby, R., Sadeh, M., Ben-Bassat, H., and Mitrani-Rosenbaum, S. (2005) *Biochem. Biophys. Res. Commun.* **328,** 221–226
25. Huizing, M., Rakocevic, G., Sparks, S. E., Mamali, I., Shatunov, A., Goldfarb, L., Krasnewich, D., Gahl, W. A., and Dalakas, M. C. (2004) *Mol. Genet. Metab.* **81,** 196–202
26. Broccolini, A., Gliubizzi, C., Pavoni, E., Gidaro, T., Morosetti, R., Sciandra, F., Giardina, B., Tonali, P., Ricci, E., Brancaccio, A., and Mirabella, M. (2005) *Neuromuscul. Disord.* **15,** 177–184
27. Krause, S., Hinderlich, S., Amsili, S., Horstkorte, R., Wiendl, H., Argov, Z., Mitrani-Rosenbaum, S., and Lochmüller, H. (2005) *Exp. Cell Res.* **304,** 365–379
28. Nakano, J., Mohan Raj, B. K., Asagami, C., and Lloyd, K. O. (1996) *J. Invest. Dermatol.* **107,** 543–548
29. Shamblott, M. J., Axelman, J., Littlefield, J. W., Blumenthal, P. D., Huggins, G. R., Cui, Y., Cheng, L., and Gearhart, J. D. (2001) *Proc. Natl. Acad. Sci. U. S. A.* **98,** 113–118
30. Jourdian, G. W., Dean, L., and Roseman, S. (1971) *J. Biol. Chem.* **246,** 430–435
31. Jones, M. B., Teng, H., Rhee, J. K., Baskaran, G., Lahar, N., and Yarema, K. J. (2004) *Biotechnol. Bioeng.* **85,** 394–405
32. Aerts, J. L., Gonzales, M. I., and Topalian, S. L. (2004) *BioTechniques* **36,** 84–91
33. Rozen, S., and Skalesky, H. J. (2000) in *Bioinformatics Methods and Protocols: Methods in Molecular Biology* (Krawetz, S., and Misener, S., eds) pp. 365–386, Humana Press, Totowa, NJ
34. Morrison, T. B., Weis, J. J., and Wittwer, C. T. (1998) *BioTechniques* **24,** 954–958
35. Chen, H. Y., Challa, A. K., and Varki, A. (2006) *J. Biol. Chem.* **281,** 7825–7833
36. Lovat, P. E., Di Sano, F., Corazzari, M., Fazi, B., Donnorso, R. P., Pearson, A. D., Hall, A. G., Redfern, C. P., and Piacentini, M. (2004) *J. Natl. Cancer Inst.* **96,** 1288–1299
37. Siddiqui, R. A., Jenski, L. J., Harvey, K. A., Wiesehan, J. D., Stillwell, W., and Zaloga, G. P. (2003) *Biochem. J.* **371,** 621–629
38. Cen, S., Guo, F., Niu, M., Saadatmand, J., Deflassieux, J., and Kleiman, L. (2004) *J. Biol. Chem.* **279,** 33177–33184
39. Kim, E. J., Sampathkumar, S.-G., Jones, M. B., Rhee, J. K., Baskaran, G., and Yarema, K. J. (2004) *J. Biol. Chem.* **279,** 18342–18352
40. Kim, E. J., Jones, M. B., Rhee, J. K., Sampathkumar, S.-G., and Yarema, K. J. (2004) *Biotechnol. Prog.* **20,** 1674–1682
41. Furukawa, K., Thampoe, I. J., Yamaguchi, H., and Lloyd, K. O. (1989) *J. Immunol.* **142,** 848–854
42. Schwarzmann, G., Hoffmann-Bleihauer, P., Schubert, J., Sandhoff, K., and Marsh, D. (1983) *Biochemistry* **22,** 5041–5048
43. Li, A., Wang, Z., Murrell, M. M., Cameron, B., Baskaran, G., Stamatos, N. M., Mao, H.-Q., and Yarema, K. J. (2004) *Glycobiology* **14,** 1150
44. Lu, P. Y., Xie, F., and Woodle, M. C. (2005) *Adv. Genet.* **54,** 117–142
45. Pekarik, V. (2005) *Brain Res. Bull.* **68,** 115–120
46. Jackson, A. L., Bartz, S. R., Schelter, J., Kobayashi, S. V., Burchard, J., Mao, M., Li, B., Carvet, G., and Linsley, P. S. (2003) *Nat. Biotechnol.* **21,** 635–637
47. Zou, W., Borrelli, S., Gilbert, M., Liu, T., Pon, R. A., and Jennings, H. J. (2004) *J. Biol. Chem.* **279,** 25390–25399
48. Kamimura, Y., Furukawa, K., Kittaka, D., Nishio, M., Hamamura, K., Fukumoto, S., and Furukawa, K. (2005) *Int. J. Oncol.* **26,** 337–344
49. Chefalo, P., Pan, Y., Nagy, N., Guo, Z., and Harding, C. V. (2006) *Biochemistry* **45,** 3733–3739
50. Saqr, H. E., Omran, O., Dasgupta, S., Yu, R. K., Oblinger, J. L., and Yates, A. J. (2006) *J. Neurochem.* **96,** 1301–1314
51. Heffer-Lauc, M., Lauc, G., Nimrichter, L., Fromholt, S. E., and Schnaar, R. L. (2005) *Biochim. Biophys. Acta* **1686,** 200–208
52. Callies, R., Schwarzmann, G., Radsak, K., Siegert, R., and Wiegandt, H. (1977) *Eur. J. Biochem.* **80,** 425–432
53. Bhunia, A. K., Schwarzmann, G., and Chatterjee, S. (2002) *J. Biol. Chem.* **277,** 16396–16402
54. Castro-Palomino, J. C., Simon, B., Speer, O., Leist, M., and Schmidt, R. R. (2001) *Chemistry* **7,** 2178–2184
55. Chen, H. Y., and Varki, A. (2002) *J. Exp. Med.* **196,** 1529–1533
56. Malisan, F., and Testi, R. (2002) *Exp. Gerontol.* **37,** 1273–1282
57. Yamada, A., Fukumoto, E., Kamasaki, Y., Ida-Yonemochi, H., Saku, T., Fujiwara, T., and Fukumoto, S. (2005) *Arch. Oral Biol.* **50,** 393–399
58. Malisan, F., Franchi, L., Tomassini, B., Ventura, N., Condo, I., Rippo, M. R., Rufini, A., Liberati, L., Nachtigall, C., Kniep, B., and Testi, R. (2002) *J. Exp. Med.* **196,** 1535–1541
59. Chung, T.-W., Choi, H.-J., Lee, Y.-C., and Kim, C.-H. (2005) *Glycobiology* **15,** 233–244
60. Moon, S.-K., Kim, H.-M., Lee, Y.-C., and Kim, C.-H. (2004) *J. Biol. Chem.* **279,** 33063–33070
61. Fukumoto, S., Mutoh, T., Hasegawa, T., Miyazaki, H., Okada, M., Goto, G., Furukawa, K., Urano, T., and Furukawa, K. (2000) *J. Biol. Chem.* **275,** 5838–5838
62. Oetke, C., Hinderlich, S., Reutter, W., and Pawlita, M. (2003) *Biochem. Biophys. Res. Commun.* **308,** 892–898
63. Malisan, F., and Testi, R. (2005) *IUBMB Life* **57,** 477–482
64. Pilkington, G. J. (2005) *Cell Prolif.* **38,** 423–433
65. Tessitore, A., del P. Martin, M., Sano, R., Ma, Y., Mann, L., Ingrassia, A., Laywell, E., Steindler, D., Hendershot, L., and d'Azzo, A. (2004) *Mol. Cell* **15,** 753–766
66. Di Sano, F., Ferraro, E., Tufi, R., Achsel, T., Piacentini, M., and Cecconi, F. (2006) *J. Biol. Chem.* **281,** 2693–2700
67. Aoki, T., Koike, T., Nakano, T., Shibahara, K., Kondo, S., Kikuchi, H., and Honjo, T. (1997) *J. Biochem.* (*Tokyo*) **121,** 122–127
68. Schuit, F., Flamez, D., De Vos, A., and Pipeleers, D. (2002) *Diabetes* **51,** S326–S332
69. Villaviecencio-Lorini, P., Laabs, S., Danker, K., Reutter, W., and Horstkorte, R. (2002) *J. Mol. Med.* **80,** 671–677
70. Hakomori, S.-I. (2002) *Proc. Natl. Acad. Sci. U. S. A.* **99,** 225–232
71. Hakomori, S. (2004) *An. Acad. Bras. Ciênc.* **76,** 553–572
72. Hakomori, S. (2004) *Glycoconj. J.* **21,** 125–137
73. Mitsuzuka, K., Handa, K., Satoh, M., Arai, Y., and Hakomori, S. (2005) *J. Biol. Chem.* **280,** 35545–35553
74. Toledo, M. S., Suzuki, E., Handa, K., and Hakomori, S. (2004) *J. Biol. Chem.* **279,** 34655–34664
75. Livak, K. J., and Schmittgen, T. D. (2001) *Methods (Amst.)* **25,** 402–408